

Available online at [www.sciencedirect.com](http://www.sciencedirect.com)

SciVerse ScienceDirect

journal homepage: [www.elsevier.com/locate/he](http://www.elsevier.com/locate/he)

# CO preferential oxidation on cordierite monoliths coated with Co/CeO<sub>2</sub> catalysts

Leticia E. Gómez, Inés S. Tiscornia, Alicia V. Boix, Eduardo E. Miró\*

Instituto de Investigaciones en Catálisis y Petroquímica, INCAPE (FIQ UNL-CONICET), Santiago del Estero 2829, (3000) Santa Fe, Argentina

## ARTICLE INFO

### Article history:

Received 7 September 2011

Received in revised form

28 December 2011

Accepted 31 January 2012

Available online xxx

### Keywords:

Co/CeO<sub>2</sub>

Monolithic catalysts

CO preferential oxidation

Co<sub>3</sub>O<sub>4</sub>

## ABSTRACT

Cordierite monoliths washcoated with Co/CeO<sub>2</sub> catalysts prepared from different methods were studied for the CO preferential oxidation reaction. Powder catalysts were also studied for the sake of comparison and in order to select the best formulations to prepare the catalytic coatings. High –Co loaded catalysts resulted in good CO conversions and they showed Co<sub>3</sub>O<sub>4</sub> as the main cobalt containing phase. Consequently, three cordierite – washcoated catalysts were prepared with high Co loadings (ca. 10 wt. % of Co in the catalytic layer). C1 and C2 were obtained by CeO<sub>2</sub> washcoating followed by cobalt impregnation. In the first case, Ce oxide particles were obtained from a nitrate solution and in the second, a Nyacol suspension was used. A third sample was prepared (C3) using a slurry of a co-precipitated Co10(CP) catalyst. Monolith C3 showed the best CO conversion, although the difference with the other catalysts was not so evident as the one observed for the powder formulations. The mechanical stability, measured by ultrasound tests, was good for all monolithic catalysts and monolith C1 showed no-deactivation after 100 h of time-on-stream at 190 °C. The structured catalysts prepared were characterized by XRD, TPR, LRS, SEM and XPS, showing that their physical-chemistry features depend on the preparation method and Co loading.

Copyright © 2012, Hydrogen Energy Publications, LLC. Published by Elsevier Ltd. All rights reserved.

## 1. Introduction

The last few years have witnessed the surge of a renewed interest in the CO oxidation reaction due to its application to the purification of hydrogen to be used in power cells [1]. While most studies concerning CO preferential oxidation have been performed using powder catalysts, it is recognized that structured catalysts are necessary in this type of reactions for practical applications [2]. In this vein, the activity and stability of monolithic catalysts have been topics of recently published research work [3–5]. It is important to study the fundamentals of this type of catalysts since the powder–support interactions can give rise to different behaviors if compared to the powder catalysts [6].

Due to their redox properties, supported cobalt oxides have been traditionally studied for CO oxidation applications [7]. Cobalt supported on zirconia, ceria, and the mixed oxide CeO<sub>2</sub> – ZrO<sub>2</sub> resulted efficient catalysts for the CO preferential oxidation [8,9]. In a previous work [10], we reported results about CO preferential oxidation over Co/ZrO<sub>2</sub> coated monoliths. When Nyacol was used as the ZrO<sub>2</sub> source, 95% of CO conversion and 60% of selectivity were reached at 230 °C. It was also shown that the open structure of the Nyacol ZrO<sub>2</sub> coating favored the diffusion process of the reactives towards the active sites. However, this catalyst presents a somewhat low mechanical stability due to the formation of interconnected surface cracks with flake-type formations that favor the detachment of portions of the washcoat.

\* Corresponding author. Tel.: +54 342 4536861.

E-mail address: [emiro@fiq.unl.edu.ar](mailto:emiro@fiq.unl.edu.ar) (E.E. Miró).

0360-3199/\$ – see front matter Copyright © 2012, Hydrogen Energy Publications, LLC. Published by Elsevier Ltd. All rights reserved.  
doi:10.1016/j.ijhydene.2012.01.159

On the other hand, it has been shown that the combined effect of cobalt oxide and ceria strongly influences the morphological and redox properties of the composite oxides, by dispersing the  $\text{Co}_3\text{O}_4$  phase and promoting the efficiency of the  $\text{Co}^{3+}\text{--Co}^{2+}$  redox couple [11]. Thus, taking into account that practical applications of this catalyst imply the use of structured systems, the main goal of this work is to prepare and characterize  $\text{Co/CeO}_2$  washcoated monoliths using different preparation strategies in order to develop active, selective and stable structured catalysts. Powder catalysts with different Co:Ce ratios were also prepared in order to carry out preliminary studies of activity and characterization for different formulations.

The stability of selected catalysts was also studied, both using ultrasound tests (to evaluate the mechanical stability of the coatings) and time-on-stream experiments in order to assess the catalytic stability of the best catalyst under reaction conditions. The monolithic catalysts were inspected by scanning electron microscopy (SEM) in order to analyze both the morphological characteristics of the films deposited by different washcoating procedures. Monoliths and powder catalysts were also characterized by Temperature-Programmed Reduction (TPR), X-ray diffraction (XRD), Laser Raman Spectroscopy (LRS) and X-ray photoelectron spectroscopy (XPS). The activity and selectivity of both structured and powder catalysts were evaluated for the preferential CO oxidation (PROx). Finally, the results were compared with those obtained for the  $\text{Co/ZrO}_2$  system studied in our previous work [10].

## 2. Experimental

### 2.1. Powder catalysts preparation

In order to perform preliminary studies, and to compare with monolithic catalysts, a series of  $\text{Co/CeO}_2$  catalysts were prepared using different Co:Ce ratios and preparation methods.  $\text{Co10(WI)}$  was prepared by the wet impregnation method with a load of cobalt of 10 wt. %, using an aqueous solution of  $\text{Co(NO}_3)_2$  and powder  $\text{CeO}_2$  obtained by precipitation of  $\text{Ce(NO}_3)_3$  with  $\text{NH}_4\text{(OH)}$  as the support. The mixture was evaporated under continuous agitation at 50 °C until achieving a paste, which was placed in the oven overnight.

$\text{Co10(CP)}$  and  $\text{Co1(CP)}$  were prepared by means of the co-precipitation method carried out by adding  $\text{NH}_4\text{(OH)}$  drop by drop into a solution of Co and Ce nitrates under vigorous stirring. The resulting precipitate was filtered and washed several times with distilled water. Then, it was dried overnight and calcined in air at 500 °C. In this way, samples with 1 and 10 wt. % of cobalt were obtained.

### 2.2. Monolithic catalysts preparation

Cordierite honeycomb monoliths (Corning, 400 cpi, 0.1 mm wall thickness),  $2\text{MgO--}2\text{Al}_2\text{O}_3\text{--}5\text{SiO}_2$ , were used as substrates. These supports had an average size of 1 cm × 1 cm × 2 cm. The active phases were deposited by the washcoating method, using different start-up suspensions.

The monolithic samples denoted as C1 and C2 were prepared from a slurry composed of the  $\text{CeO}_2$  powder

suspended in distilled water or from a commercial suspension (Nyacol) consisting in particles of about 20 nm stabilized in an acetic acid solution, respectively. A series of impregnations were carried out until an adequate ceria layer was obtained. After each immersion cycle, the suspension excess was removed by blowing air through the channels of the monolith. After that, cobalt was incorporated by means of successive impregnations of the monoliths in a  $\text{Co(NO}_3)_2$  solution. Sample C3 was prepared from an aqueous suspension of the pre-formed powder  $\text{Co10(CP)}$ .

After the washcoating and air blowing processes, all monoliths were calcined in air flow at 500 °C. The adherence of the catalytic films was evaluated using a method described in the patent literature [12] with an ultrasonic treatment. The weight of the sample both before and after the ultrasonic treatment was measured.

### 2.3. Catalytic tests

Preferential CO oxidation experiments were performed in a fixed-bed flow reactor. Powder samples were placed in a tubular quartz reactor (8 mm i.d.) and monolithic samples were placed in a tubular quartz reactor (19 mm o.d.). The reaction mixture consisted of CO 1%,  $\text{O}_2$  1% and  $\text{H}_2$  40%, He balance. The weight/total flow ratio was adjusted to  $2.1 \text{ mg}\cdot\text{cm}^{-3} \text{ min}$  by means of mass flow controllers.

The CO conversion and the selectivity towards  $\text{CO}_2$  were defined as:

$$C_{\text{CO}} = (1 - [\text{CO}]/[\text{CO}]^0) \cdot 100$$

$$S = [\text{CO}_2]/2 \cdot ([\text{O}_2]^0 - [\text{O}_2]) \cdot 100$$

where  $[\text{CO}]$ ,  $[\text{CO}_2]$  and  $[\text{O}_2]$  were reactor exit concentrations and  $[\text{CO}]^0$ ,  $[\text{O}_2]^0$  represented feed concentrations, which were measured with a chromatograph GC-2014 Shimadzu equipped with a TCD cell. All the catalysts were pretreated during 1 h in oxygen at 300 °C before the catalytic test.

### 2.4. Catalysts characterization of powder and monolithic samples

#### 2.4.1. X-ray Diffraction (XRD)

Powder and monolithic catalysts were characterized by XRD in a Shimadzu XD-D1 diffractometer with monochromator using  $\text{Cu-K}\alpha$  ( $\lambda = 1.542 \text{ \AA}$ ) radiation at 30 kV and 40 mA. The scan rate was  $1^\circ \cdot \text{min}^{-1}$  in the range  $2\theta = 20\text{--}80^\circ$ .

#### 2.4.2. Temperature-programmed reduction

$\text{H}_2$  - TPR experiments were performed with an OKHURA TP-2002S instrument equipped with a TCD detector on samples of 100 mg in a 5%  $\text{H}_2/\text{Ar}$  gas mixture using a temperature ramp rate of  $10^\circ \text{C min}^{-1}$ . Prior to the TPR analysis, the samples were treated at 300 °C for 30 min under nitrogen flow to clean the surface.

#### 2.4.3. X-ray Photoelectron Spectroscopy

XPS analyses were performed in a multi-technique system (SPECS) equipped with a dual Mg/Al X-ray source and hemispherical PHOIBOS 150 analyzer operating in the fixed

analyzer transmission (FAT) mode. The spectra were obtained with pass energy of 30 eV, the Al K $\alpha$  X-ray source ( $h\nu = 1486.6$  eV) was operated at 100W. The spectra regions corresponding to Co 2p, O 1s, Ce 3d and C 1s (reference 284.6 eV) core levels were recorded for each sample. The data treatment was performed with the Casa XPS program (Casa Software Ltda., UK).

#### 2.4.4. Laser Raman Spectroscopy

LRS spectra were acquired using a Horiba JOBIN YVON Lab RAM HR instrument. The excitation source was the 514.5 nm line of a Spectra 9000 Photometrics Ar ion laser with the laser power set at 30 mW. Spectra were collected under atmospheric conditions on calcined C1 and C2 monoliths.

#### 2.4.5. Microscopic observations

Morphologies of monolithic films were examined using a scanning electron microscope JEOL JSM-35C instrument equipped with an electron acquisition imaging system operated a 20 kV. The samples were covered with a thin gold layer to improve the images.

## 3. Results and discussion

### 3.1. Catalytic evaluations

Three powder catalysts and the same number of monolithic catalysts were evaluated for the CO preferential oxidation. In order to select the characteristics of the Co/CeO<sub>2</sub> used for the washcoating of the cordierite monoliths, powder catalysts were prepared under different conditions and evaluated for the reaction under study (Table 1).

The three monolithic catalysts showed good stability of the coating since a low weight loss was measured after the ultrasound test. Moreover, in a previous work [10] we showed that after the washcoating there is some amount of material that is loosely adhered to the monolith, which is easily lost after the first ultrasound treatment. However, the remaining material is firmly attached and is mechanically stable.

Fig. 1A shows CO conversions for the different Co/CeO<sub>2</sub> powder samples, and they are compared with a Co/ZrO<sub>2</sub> catalyst with a similar Co loading. It can be seen that the co-precipitated sample (CP) with high-cobalt loading displays the highest activity, reaching almost total CO conversion at 160 °C, while the impregnated sample (WI) reaches the same conversion but at a somewhat higher temperature. For the solid solution CoO<sub>x</sub> – CeO<sub>2</sub> with low cobalt loading, total CO

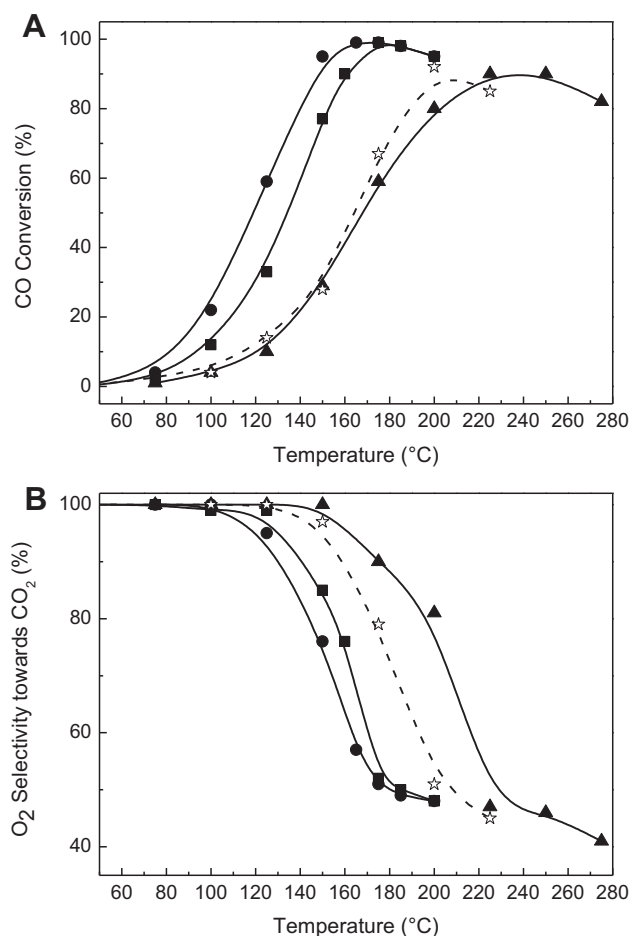


**Fig. 1 – Catalytic evaluation of powder catalysts. (A) CO conversion (B) Selectivity of O<sub>2</sub> to CO<sub>2</sub>. Reaction conditions: 1% CO, 1% O<sub>2</sub>, 40% H<sub>2</sub> in He balance. Catalyst weight/total flow: 2.1 mg cm<sup>-3</sup> min ■ Co10(WI), ● Co10(CP), ▲ Co1(CP), ☆ Co10/ZrO<sub>2</sub> powder.**

conversion is not reached, showing a maximum value of 85% at a considerable higher temperature of about 240 °C. This result does not mean that segregated Co oxide has a better specific activity compared with the solid solution. A more rigorous kinetic study is necessary to gain further insight into this aspect. Nevertheless, we decided to prepare the monolithic catalysts with high loadings of Co in order to secure the presence of the Co<sub>3</sub>O<sub>4</sub> phase. In the same figure it can be observed that a Co/ZrO<sub>2</sub> catalyst with 10 wt. % of Co loading reaches 95%

**Table 1 – Conditions for monolithic catalysts preparation.**

Monolith	Slurry composition	Support weight Gained (wt.%)	Co (wt.%) <sup>a</sup>	Weight loss (wt. %) <sup>b</sup>
C1	CeO <sub>2</sub> /H <sub>2</sub> O (10 wt.%)	10.2	11.2	1.7
C2	Nyacol CeO <sub>2</sub> (20 wt. %)	19.8	10.1	0.7
C3	Co10(CP)/H <sub>2</sub> O (10 wt. %)	13.0	10.0	1.6

<sup>a</sup> Calculated from Co/CeO<sub>2</sub> catalyst film.

<sup>b</sup> Calculated from total weight of monolith.

of CO conversion at 200 °C, indicating that CeO<sub>2</sub> is a better support than ZrO<sub>2</sub> for high loaded Co catalysts. In Fig. 1B, the selectivities of oxygen towards CO<sub>2</sub> are displayed, showing a value of approximately 50% when CO conversions are at the maximum value for each sample.

Fig. 2A and B shows the catalytic results obtained with monolithic catalysts. Surprisingly, the three samples employed do not differ considerably in CO conversions and selectivity behaviors. Almost total CO conversion is reached at 200 °C, temperature considerably higher than that obtained for the powders with high Co loadings. These results would suggest that mass transfer limitations at the gas-coating interphase and/or inside the coating layer are playing an important role. For comparison, CO conversions for a monolith coated with Co/ZrO<sub>2</sub> is also depicted in Fig. 2B, showing that for this sample a high CO conversion is also obtained but at 240 °C. The selectivity behaviors are totally different, while the Co/ZrO<sub>2</sub> coated monolith shows a volcano – shaped behavior, reaching a maximum value of about 80%. In the case of the Co/CeO<sub>2</sub> coatings, the selectivities remain constant at 100% until ca. 150 °C and from this value on, as temperature increases selectivity continuously decreases.

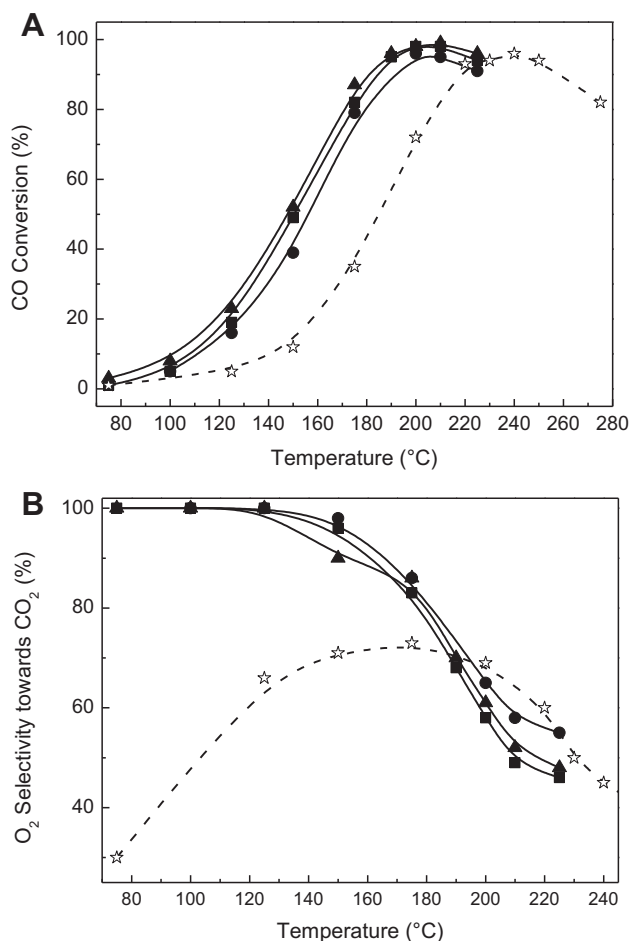


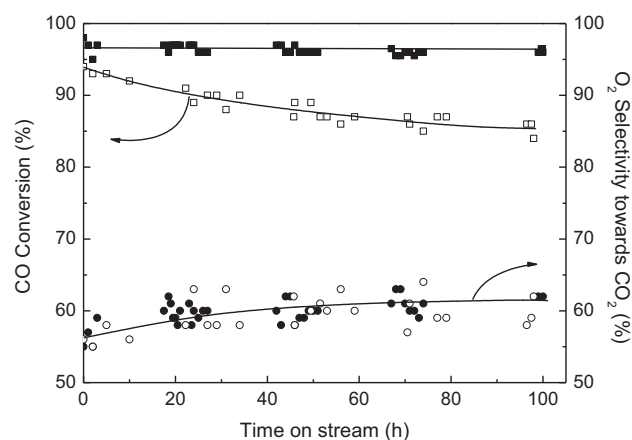
**Fig. 2 – Catalytic evaluation of monolithic catalysts. (A) CO conversion (B) Selectivity of O<sub>2</sub> to CO<sub>2</sub>.** Reaction conditions: 1% CO, 1% O<sub>2</sub>, 40% H<sub>2</sub> in He balance. Catalyst weight/total flow: 2.1 mg cm<sup>-3</sup> min ■ C1, ● C2, ▲ C3, ☆ Co/ZrO<sub>2</sub> monolith.

The monolithic C1 catalyst was subjected to a stability test under reaction conditions. Fig. 3 shows that after 100 h of time-on-stream at 190 °C, the CO conversion is constant at about 96%, while the selectivity towards CO<sub>2</sub> increases from 55% to 63%. This behavior is better than that obtained for the Co/ZrO<sub>2</sub> monolithic catalyst at 240 °C, which is also shown in Fig. 3, where it can be seen that after 100 h of TOS the CO conversion decreases from 95 to 85%, while the selectivity towards CO<sub>2</sub> increases from 55 to 60%. Thus, comparing monolithic catalysts, the coating of Co/CeO<sub>2</sub> is better than that made of Co/ZrO<sub>2</sub>, showing higher activity and stability while maintaining a similar selectivity towards CO<sub>2</sub>.

### 3.2. Catalysts characterization

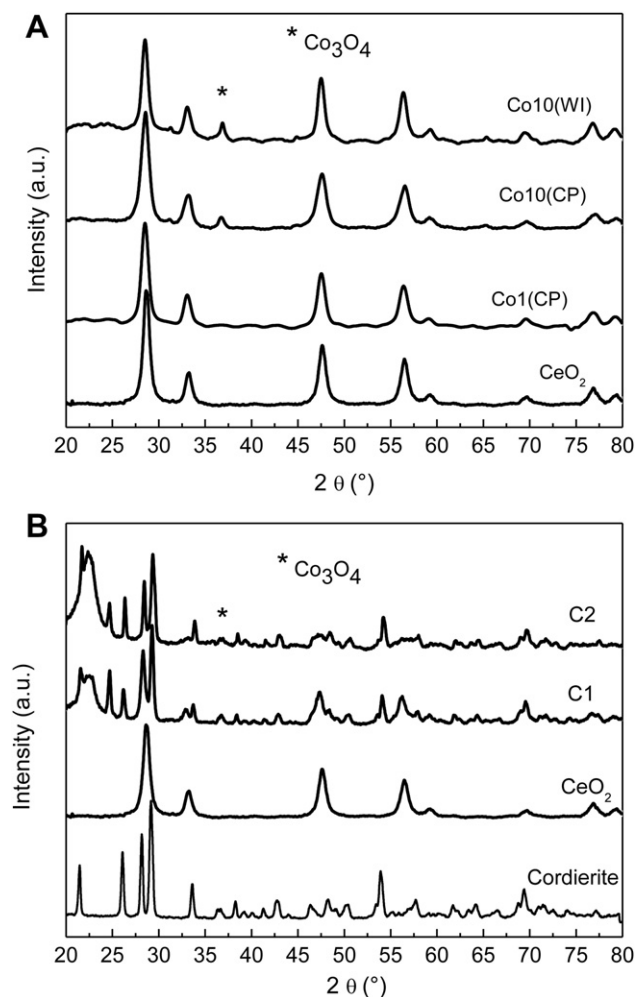
XRD patterns of calcined powder catalysts and CeO<sub>2</sub> support are illustrated in Fig. 4A. It can be observed that the cubic structure of CeO<sub>2</sub> appears with its characteristic peaks. Besides the ceria signals, in the Co10(CP) and Co10(WI) samples, the main peak of the Co<sub>3</sub>O<sub>4</sub> phase is identified at 36.8° [8,13]. The remaining signals of the spinel (31.3°, 44.9°, 59.4° and 64.9°) are weaker and cannot be clearly identified. In sample Co10(CP), all signals are broader than those of Co10(WI), indicating that probably the size particle of the CeO<sub>2</sub> phase was smaller in the first preparation. For the Co1(CP) sample, the diffractogram was similar to CeO<sub>2</sub> and Co<sub>3</sub>O<sub>4</sub> peaks were not found, suggesting the formation of a solid solution, which is the most probable structure taking into account that the cobalt wt. % is below the saturation limit for cobalt – ceria solid solutions, as reported by Wang et al. [14].

Fig. 4B presents XRD patterns of calcined monoliths C1 and C2; ceria powder and bare cordierite are also included for comparison. The most visible signals correspond to CeO<sub>2</sub> and cordierite diffractograms. However, a weak signal is observed at 36.8 °C which might correspond to the Co<sub>3</sub>O<sub>4</sub> phase. This results suggests that cobalt oxide is better dispersed in monolithic samples, which is in agreement with the results reported in [10] for Co/ZrO<sub>2</sub> coated in cordierite monoliths.



**Fig. 3 – Long term stability test for COPROX on C1 monolithic catalyst at 190 °C (■ ●) and Co/ZrO<sub>2</sub> monolithic catalyst at 240 °C (□ ○).** Reaction conditions: 1% CO, 1% O<sub>2</sub>, 40% H<sub>2</sub> in He balance. Catalyst weight/total flow: 2.1 mg cm<sup>-3</sup> min.





**Fig. 4 – XRD patterns: (A) Calcined  $\text{CeO}_2$  and Co10(WI), Co10(CP), Co1(CP) powder catalyst. (B) Cordierite,  $\text{CeO}_2$  powder, C1 and C2.**

Fig. 5 shows the Raman spectra of C1 and C2 monoliths and that of bare cordierite. The  $\text{CeO}_2$  spectrum, also included for comparison, shows a single peak at  $464\text{ cm}^{-1}$ . The bands at 193, 484, 524, 615 and  $680\text{ cm}^{-1}$  that are seen in C1 and C2 samples can be safely assigned to the vibrations of the  $\text{Co}_3\text{O}_4$  spinel [13,15]. Despite the high ceria loading, all the samples prepared from different ceria sources showed only a weak signal belonging to  $\text{CeO}_2$ , this peak being a bit more intense in monolith C2 than in C1. This effect could be ascribed to the presence of Co cations in  $\text{CeO}_2$ , generating a structural deformation and thus a decrease in the peak intensity in the Raman spectra, in agreement with that reported by Liu et al. [13].

The SEM micrographs in Fig. 6 show the structure and surface morphology of the catalytic films washcoated on monoliths C1 and C2. The pictures reveal that the coating of Co/ $\text{CeO}_2$  in both samples is homogeneously deposited all along the channels length. Fig. 6A shows the film deposited on C2. The coating exhibits an arrangement of interconnected surface cracks and a mosaic-type structure. The formation of flakes and cracks can be attributed to a combination of

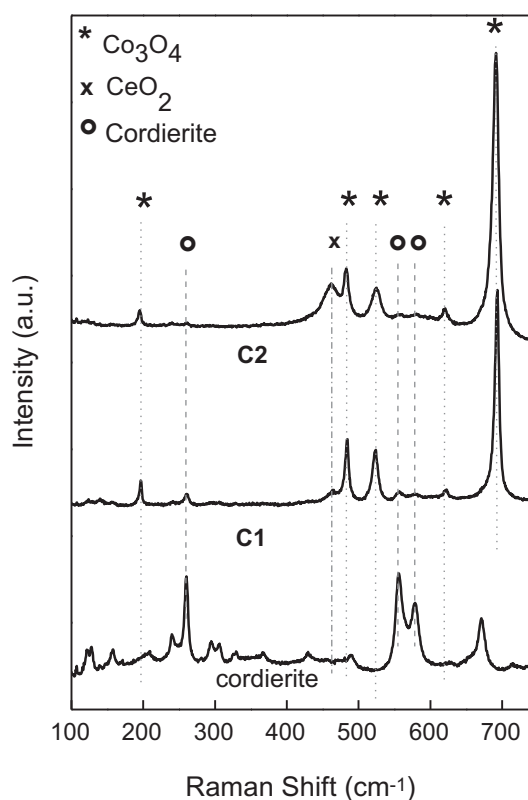


**Fig. 5 – Laser Raman Spectroscopy (LRS). Spectra of C1 and C2 monoliths and cordierite.**

different phenomena involved during the drying and calcination process, such as solvent removal, the shrinkage of hydrated  $\text{CeO}_2$  particles and suspension stabilizer combustion, as reported by Banús et al. [16]. On the other hand, Fig. 6B shows a smooth superficial Co/ $\text{CeO}_2$  coverage corresponding to the C1 sample. Despite these differences in coating structures, CO conversions and selectivities towards  $\text{CO}_2$  were similar in both samples, as shown in Fig. 2 above.

TPR experiments over powder and monolith samples were carried out with the aim to study the reducibility of samples when ceria is used as support. The  $\text{H}_2$ -TPR profiles of powder and monolithic catalysts are displayed in Fig. 7A and B, respectively. TPR curves of powder Co10(CP) and Co10(WI) show two well defined peaks in the 240–450 °C temperature range. According to the literature, the low temperature reduction peak is assigned to the reduction of  $\text{Co}^{3+}$  to  $\text{Co}^{2+}$  at the interface between  $\text{Co}_3\text{O}_4$  and  $\text{CeO}_2$  while the other peak is assigned to the reduction of  $\text{Co}^{2+}$  to metallic cobalt [11,15]. In our previous work [10], these two peaks appeared at higher temperatures when the support used was  $\text{ZrO}_2$ . In this way, it is shown that the presence of ceria improves the reducibility of cobalt, which could be the reason for the higher activity of the cobalt – ceria catalyst. The lower reduction temperatures obtained for cobalt species reduction when ceria is used as support might be related to the distortion that cobalt ions provoke when they are introduced in the ceria lattice. A charge unbalance and lattice distortion occurs in the  $\text{CeO}_2$  structure which leads to the generation of oxygen vacancies.

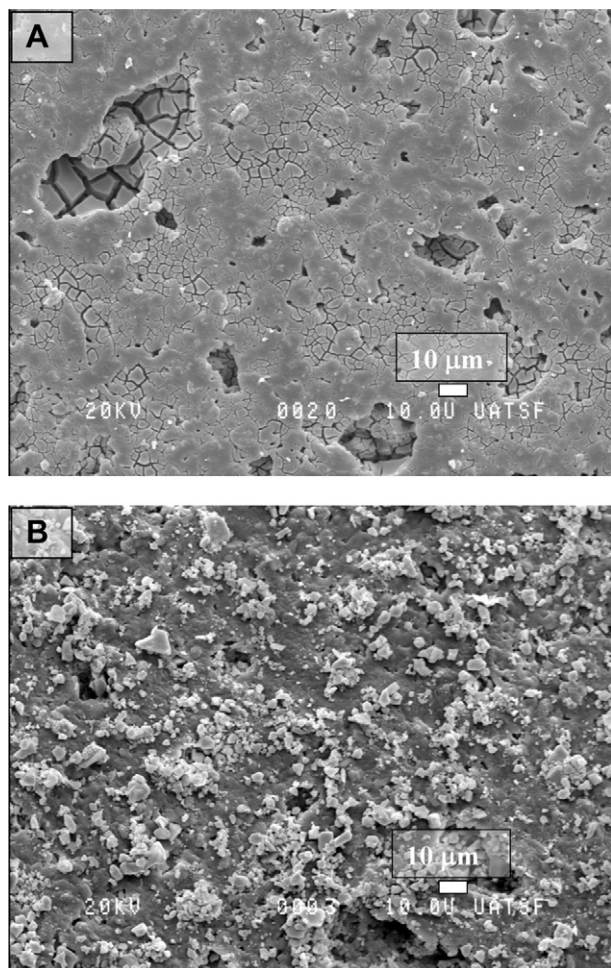


Fig. 6 – SEM micrographs of coated monoliths (A) C2, (B) C1.

These vacancies bond more weakly to oxygen species and they can be thus reduced at lower temperatures [14].

With respect to the reduction of Ce species, several authors coincide in reporting two peaks for the reduction of ceria support [14,15,17], one of them centered at about 500 °C which corresponds to the superficial oxygen reduction, and the second peak at about 850 °C which is related to the reduction of bulk oxygen species. In the Co10(CP) profile, a peak at 471 °C is observed. This signal might be attributed to the reduction of surface species of the support, but a shift at lower temperatures is produced. Probably the intimate contact between cobalt species and cerium oxide enhances the ceria reducibility. On the other hand, in the Co10(WI) sample, this peak is either not observed or present as a small shoulder, suggesting that the preparation method strongly influences the reducibility of the catalysts. It is reasonable that for the co-precipitated sample a more intimate contact between Co and Ce oxides is obtained, thus provoking an increased reducibility due to a synergic effect. Since the redox behavior is an important factor in determining the catalytic activity for the reaction under study, this result is in line with the somewhat higher activity of the CP catalyst when compared with the WI one. As a matter of fact, as discussed by Liotta et al. [11], the lower the reduction temperature the stronger

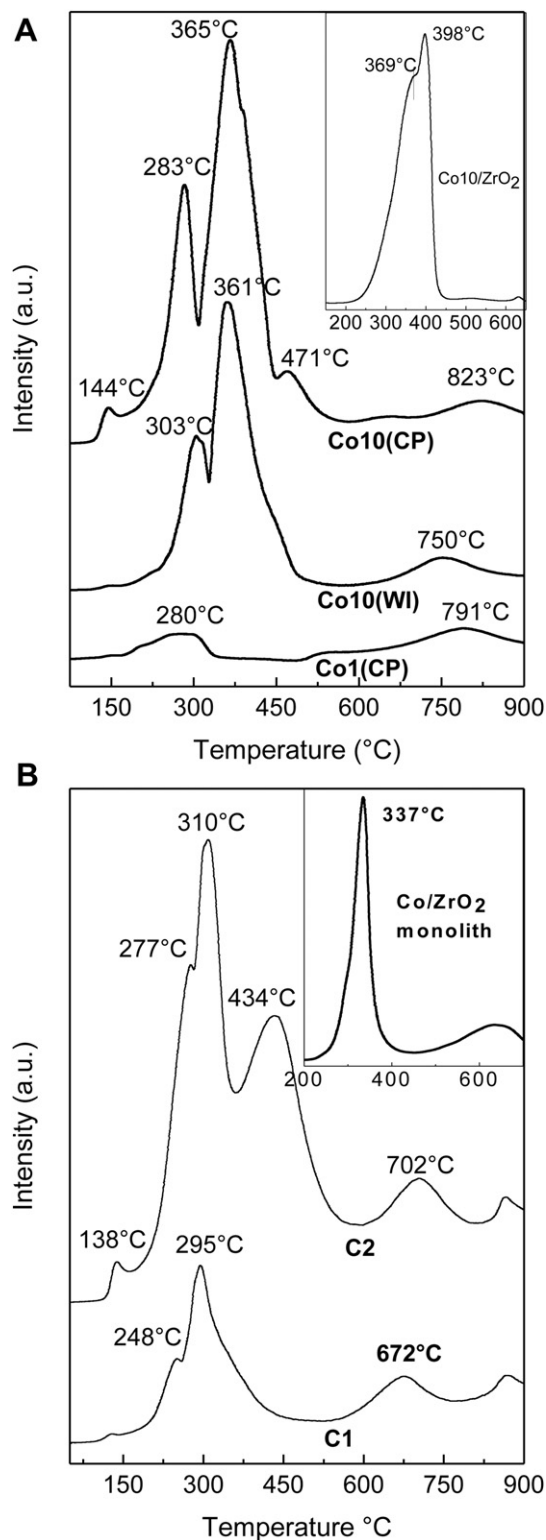


Fig. 7 – Reducibility of catalysts measured by temperature programmed reduction. (A) Co10(CP), Co10(WI) and Co1(CP) powder catalysts. (B) C1 and C2 monolithic catalysts.

the redox capacity of the catalysts. The mobility of surface oxygen species in ceria is high compared to other conventional oxides such as  $\text{ZrO}_2$  and  $\text{SiO}_2$  and this mobility helps in the removal of lattice oxygen during the reduction process. It

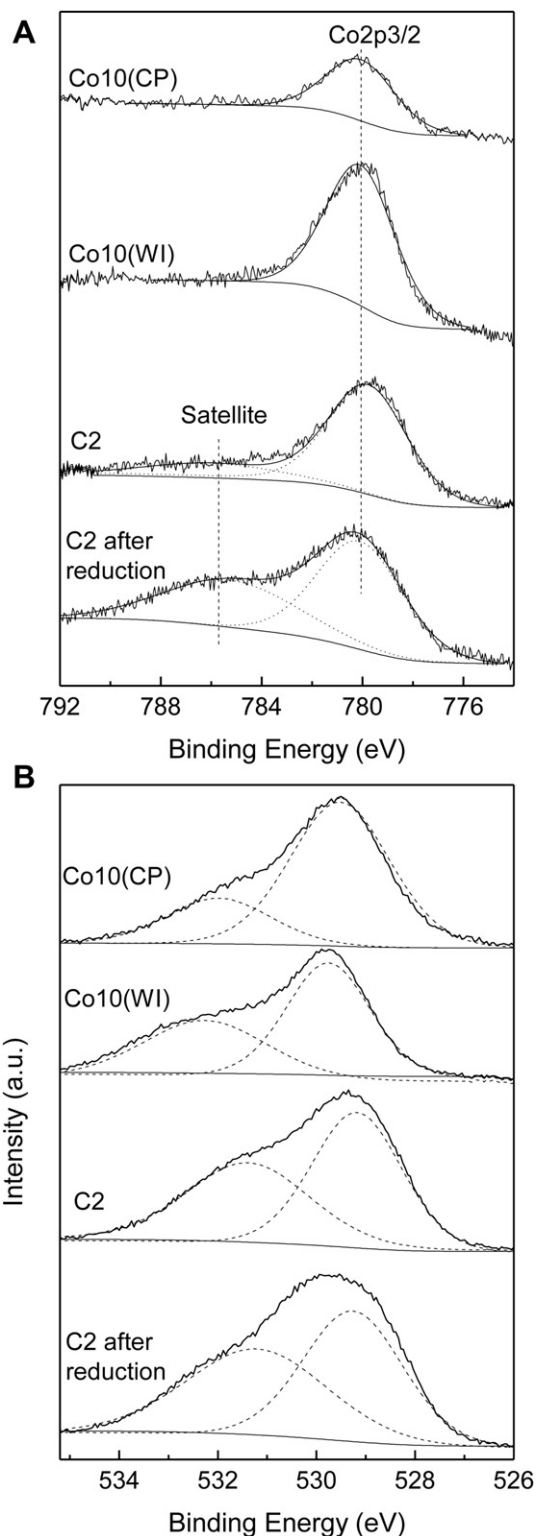
has been reported in the literature that the oxidative performance of  $\text{Co}_3\text{O}_4$  follows a redox mechanism which involves reduction/oxidation of  $\text{Co}^{3+}$  site. The presence of ceria and the synergism with cobalt would improve its reducibility. In the case of the Co1(CP) catalyst, the TPR profile shows that the feature of the  $\text{CeO}_2$  bulk is higher than that of surface species, suggesting that for low-loaded Co/ $\text{CeO}_2$  the synergic effect is lower, in agreement with Liotta et al. [11].

Fig. 7B shows the reduction curves for monolithic catalysts. Two overlapped reduction peaks corresponding to the reduction of  $\text{Co}_3\text{O}_4$  occurred instead of the two splitting peaks observed in powder samples. Luo et al. [15] proposed that this behavior might be related to particle size, by which large particles of  $\text{Co}_3\text{O}_4$  are reduced directly to metallic Co in a single step while small particles that interact with ceria were reduced in two steps. However, in agreement with what was reported in a previous work for the Co/ $\text{ZrO}_2$  catalyst, a shift to lower reduction temperatures of the  $\text{Co}_3\text{O}_4$  reduction peak occurs in monoliths with respect to the powder catalyst. This behavior might be attributed to well-dispersed catalytic particles in the cordierite structure, which is in line with the XRD results shown above. Thus, the presence of two overlapped reduction signals could be attributed to interactions with the cordierite monolith rather than to the particle size.

The mobility of surface oxygen species in ceria is high compared to other conventional oxides, we calculated the reduction degree of the  $\text{Ce}^{4+}$  towards  $\text{Ce}^{3+}$  process considering that all  $\text{Co}_3\text{O}_4$  was reduced to  $\text{Co}^0$ . While for Co10(WI), the said degree was 52%, for Co10(CP) it was completely reduced, again indicating that a better contact between oxide phases is obtained for the CP catalyst.

The XPS surface analysis was performed over Co10(CP) and Co10(WI) powders and C2 monolithic catalysts. The spectra for Co  $2p_{3/2}$  and O 1s regions are presented in Fig. 8. In all samples the Co  $2p_{3/2}$  peak position was found around  $780.0 \pm 0.1$  eV (Table 2), with a spin-orbit splitting at 795.0 eV corresponding to the Co  $2p_{3/2}$  peak. The binding energy of the main peak may correspond to either  $\text{Co}^{2+}$  or  $\text{Co}^{3+}$  species since binding energy differences are negligible for both species. It is known that the XP spectrum of the  $\text{Co}^{2+}$  compound exhibits a pronounced satellite peak on the high-energy binding energy side of main peak. This satellite is not present in the diamagnetic  $\text{Co}^{3+}$  compound [7,11]. Fig. 8A shows a small satellite peak at 786.0 eV in the C2 monolithic catalyst. The satellite peak intensity significantly increased after reducing the catalyst in  $\text{H}_2$  flow for 10 min inside the pretreatment chamber of the spectrometer, which is indicative of the reduction of  $\text{Co}^{3+}$  to  $\text{Co}^{2+}$  species, in agreement with the TPR results. Thus the  $I_{\text{sat}}/I_{\text{mp}}$  ratio might be indicative of the oxidation state of cobalt species, which change from 0.1 to 0.6 when the C2 monolith is reduced. The absence of the satellite peak in powder samples would indicate that  $\text{Co}^{3+}$  species are dominant.

Fig. 8B shows the O 1s XP spectra for all of the catalysts studied. Broad and complex shape spectra are observed in this region for powdered and monolithic catalysts. These spectra can be described as the result of the overlapping of two components corresponding to different species or groups of species. In Co10(WI), the first peak appears at 529.8 eV and the other at 532.3 eV. Similar values are observed for the Co10(CP)



**Fig. 8 – XPS spectra of Co10(CP), Co10(WI), and C2 catalysts. (A)  $\text{Co}2p_{3/2}$  sub-region. (B) O1s region.**

sample, which shows signals at 529.5 and 532.0 eV, respectively. The O 1s peak at lower binding energy is in agreement with the proposed values for the bulk  $\text{CeO}_2$  oxide. Also, a similar value is assigned to the oxygen belonging to cobalt oxide [13,18]. The other component at higher energy is



**Table 2 – Surface features of powder and monolith catalysts. XPS data.**

Catalyst	O1s/eV (fwhm)	Co2p <sub>3/2</sub> /eV (fwhm)	Satellite/eV (fwhm)	Co/Ce <sub>surf</sub>	Co/Ce <sub>bulk</sub>
Co10(CP)	529.5 (2.4) 532.0 (2.5)	780.1 (3.2)	–	0.13	0.14
Co10(WI)	529.8 (2.0) 532.3 (3.0)	780.2 (3.2)	–	0.52	0.14
C1	527.0 (4.9) 529.7 (2.0) 532.4 (2.6)	780.0 (2.5)	–	0.06	0.15
C2	527.0 (4.9) 529.7 (2.0)	780.0 (3.7)	785.8 (3.6)	0.44	0.14
C2 after reduction	529.3 (2.4) 531.2 (3.4)	780.1 (4.0)	785.3 (6.2)	0.59	0.14

ascribed to the presence of hydroxyl, water and/or carbonate groups adsorbed on the material surface as generally described for oxide surfaces [19] (Table 2).

The spectra of the Ce 3d region show signals with binding energies (not shown) at 882.9, 888.7 and 898.5, which correspond to the Ce3d<sub>5/2</sub> level and peaks at 901.4, 907.7 and 916.9 eV, which belong to the Ce3d<sub>3/2</sub> level. These values are characteristic of Ce<sup>4+</sup> species [20]. Peaks corresponding to the final state of Ce<sup>3+</sup> were found only in the C2 monolith after reduction treatment.

#### 4. Conclusions

The cordierite monoliths washcoated with the Co/CeO<sub>2</sub> catalyst is a promising system to be used in hydrogen purification through the CO preferential oxidation process. Before the preparation of the structured catalysts, a preliminary study was conducted with powder formulations, concluding that a ceria support loaded with 10 wt. % of cobalt oxide catalysts resulted in an effective catalyst, reaching 96% CO conversion and 60% selectivity towards CO<sub>2</sub> at 190 °C for the Co10(CP) catalyst. These catalysts showed Co<sub>3</sub>O<sub>4</sub> as the main cobalt containing phase. On the contrary, low Co loadings (below the solubility limit of cobalt in CeO<sub>2</sub>) resulted in poor catalytic behavior, indicating that the segregation of Co<sub>3</sub>O<sub>4</sub> is beneficial. Comparing the high-cobalt loaded catalysts, Co10(CP) showed somewhat higher CO conversions than Co10(WI) probably due to the better redox capacity of the former. With respect to the structured solids, the three monolithic catalysts showed a similar behavior among them, but the higher CO conversion was reached at 200 °C, temperature considerably higher than those obtained for the better powder catalysts. The monolithic catalyst C1 was stable during 100 h of time-on-stream and all the prepared monoliths showed good mechanical stability after a standard ultrasound test.

#### Acknowledgements

The authors wish to acknowledge the financial support received from ANPCyT, UNL and CONICET. They are also

grateful to ANPCyT for PME Grants to finance the purchase of characterization equipment. Thanks are given to Elsa Grimaldi for the English language editing and to Claudio Maitre for his technical assistance.

#### REFERENCES

- [1] Bion N, Epron F, Moreno M, Mariño F, Duprez D. *Top Catal* 2008;51(1–4):76–88.
- [2] Avila P, Montes M, Miró EE. *Chem Eng J* 2005;109:11–36.
- [3] Arzamendi G, Uriz I, Diéguez PM, Laguna OH, Hernández WY, Álvarez A, et al. *Chem Eng J* 2011;167:588–96.
- [4] Ayastuy JL, Gamboa NK, Gonzalez-Marcos MP, Gutierrez-Ortiz MA. *Chem Eng J* 2011;171:224–31.
- [5] Divins NJ, López E, Roig M, Trifonov T, Rodríguez A, González de Rivera F, et al. *Chem Eng J* 2011;167:597–602.
- [6] Boix AV, Zamaro JM, Lombardo EA, Miró EE. *Appl Catal B Environ* 2003;46:121–32.
- [7] Kang M, Song MW, Lee CH. *Appl Catal A Gen* 2003;251:143–56.
- [8] Woods MP, Gawade P, Tan B, Ozkan US. *Appl Catal B Environ* 2010;97:28–35.
- [9] Zhao Z, Lin X, Jin R, Dai Y, Wang G. *Catal Comm* 2011;12:1448–51.
- [10] Gómez LE, Tiscornia IS, Boix AV, Miró EE. *Appl Catal A Gen* 2011;401:124–33.
- [11] Liotta LF, Di Carlo G, Pantaleo G, Venezia AM, Deganello G. *Appl Catal B Environ* 2006;66:217–27.
- [12] Yasaki D, Yoshino Y, Ihara K, Ohkubo K. US Patent 5,208,206 (1993).
- [13] Liu J, Zhao Z, Wang J, Xu C, Duan A, Jiang G, et al. *Appl Catal B Environ* 2008;84:185–95.
- [14] Wang J, Shen M, Wang J, Gao J, Ma J, Liu S. *Catal Today* 2011;175:65–71.
- [15] Luo JY, Meng M, Li X, Li XG, Zha YQ, Hu TD, et al. *J Catal* 2008;254:310–24.
- [16] Banús E, Milt V, Miró EE, Ulla MA. *Appl Catal A Gen* 2010;379(1–2):95–104.
- [17] Ranga Rao G, Mishra BG. *Bull Catal Soc India* 2003;2:122–34.
- [18] Galtayries A, Sporken R, Riga J, Blanchard G, Caudano R. *J Electron Spectrosc Relat Phenom* 1998;88–91:951–6.
- [19] Alvarez M, López T, Odriozola JA, Centeno MA, Domínguez MI, Montes M, et al. *Appl Catal B Environ* 2007;73:34–41.
- [20] Swiatowska J, Lair V, Pereira-Nabais C, Cote G, Marcus P, Chagnes A. *Appl Surf Sci* 2011;257:9110–9.